

Multiview Point Cloud Kernels for Semisupervised Learning

In semisupervised learning (SSL), we learn a predictive model from a collection of labeled data and a typically much larger collection of unlabeled data. These lecture notes present a framework called multiview point cloud regularization (MVPCR) [5], which unifies and generalizes several semisupervised kernel methods that are based on data-dependent regularization in reproducing kernel Hilbert spaces (RKHSs). Special cases of MVPCR include coregularized least squares (CoRLS) [7], [3], [6], manifold regularization (MR) [1], [8], [4], and graph-based SSL. An accompanying theorem shows how to reduce any MVPCR problem to standard supervised learning with a new *multiview kernel*.

RELEVANCE

RKHS techniques form the basis of many state-of-the-art supervised learning algorithms, such as support vector machines (SVMs), kernel ridge regression, and Gaussian processes. By plugging the new multiview kernel into these or any other standard kernel method, we can conveniently convert them to SSL algorithms. Via the reduction of MVPCR to supervised RKHS learning, we can easily derive generalization error bounds using standard results. In particular, we generalize the bound given in [6] for CoRLS. From an experimental perspective, there are many interesting algorithms that fit into the MVPCR framework that have yet to be explored. As one example, we present manifold coregularization, which directly combines the ideas in CoRLS and MR.

PROBLEM SETTING

We begin with some learning theory. For any input x from an input space \mathcal{X} , we suppose there is some target $y \in \mathbb{R}$ that we would like to predict. The “loss” incurred when we predict \hat{y} rather than y is given by a nonnegative loss function $V(\hat{y}, y)$. Our goal is to find a prediction function whose average loss, or risk, is small. More formally, we assume that (x, y) pairs are drawn from a distribution $P_{\mathcal{X} \times \mathcal{Y}}$, and the risk of f is defined as the expected loss on a random pair: $R(f) = \mathbb{E}V(f(X), Y)$. Although we would like to minimize $R(f)$, in practice we cannot even compute it since $P_{\mathcal{X} \times \mathcal{Y}}$ is unknown. Instead, suppose we have a training set of pairs $(x_1, y_1), \dots, (x_\ell, y_\ell)$ sampled independently from $P_{\mathcal{X} \times \mathcal{Y}}$. Then we can minimize the empirical risk, which is defined as $\hat{R}_\ell(f) = (1/\ell) \sum_{i=1}^\ell V(f(x_i), y_i)$. By the law of large numbers, $\lim_{\ell \rightarrow \infty} \hat{R}_\ell(f) = R(f)$ with probability one, so this is a plausible substitute. However, the minimizer of $\hat{R}_\ell(f)$ is not guaranteed to converge to the minimizer of $R(f)$ without additional constraints on the set of functions over which we are minimizing. Thus we constrain our minimization to some class of functions \mathcal{F} and define the empirical risk minimizer and risk minimizer, respectively, by $\hat{f}_\ell = \arg \min_{f \in \mathcal{F}} \hat{R}_\ell(f)$ and $f_* = \arg \min_{f \in \mathcal{F}} R(f)$. For many \mathcal{F} , we will have $R(\hat{f}_\ell) \rightarrow R(f_*)$. With a finite training set, however, there is an inevitable gap between the risk of \hat{f}_ℓ and the risk of f_* . This gap is called estimation error, since \hat{f}_ℓ is only an “estimate” of the unknown function f_* . The speed with which the estimation error converges to zero is governed, in part, by the size of the class \mathcal{F} , with smaller classes giving faster convergence. As the

ultimate performance benchmark, we consider the Bayes prediction function, defined as $y_* = \arg \min_f R(f)$, which minimizes the risk over all functions. The difference in risk between y_* (the best overall) and f_* (the best in \mathcal{F}) is called the approximation error. We can decompose the excess risk that \hat{f}_ℓ has over y_* using these two types of error:

$$R(\hat{f}_\ell) - R(y_*) = \underbrace{R(\hat{f}_\ell) - R(f_*)}_{\text{estimation error}} + \underbrace{R(f_*) - R(y_*)}_{\text{approximation error}}.$$

In practice, a convenient way to adjust the balance between approximation and estimation error is to use Tikhonov regularization, in which we solve $f_* = \arg \min_{f \in \mathcal{F}} \hat{R}_\ell(f) + \gamma \Omega(f)$, for some $\gamma > 0$ and some nonnegative penalty function Ω . As γ increases, f_* is pulled towards a minimizer of $\Omega(f)$, which effectively limits the domain of optimization. Generally speaking, increasing γ will increase approximation error and decrease estimation error. Many popular learning algorithms, including the SVM and kernel ridge regression, are Tikhonov regularization problems for which \mathcal{F} is an RKHS. An RKHS of functions from \mathcal{X} to \mathbb{R} is a Hilbert space \mathcal{H} with a reproducing kernel, i.e., a function $k: \mathcal{X} \times \mathcal{X} \rightarrow \mathbb{R}$ for which the following properties hold: a) $k(x, \cdot) \in \mathcal{H}$ for all $x \in \mathcal{X}$, and b) $\langle f, k(x, \cdot) \rangle_{\mathcal{H}} = f(x)$, for all $x \in \mathcal{X}$ and $f \in \mathcal{H}$. The most basic RKHS regularization problem is

$$\hat{f}_\ell = \arg \min_{f \in \mathcal{H}} [\hat{R}_\ell(f) + \gamma \|f\|_{\mathcal{H}}^2]. \quad (1)$$

By the representer theorem, $\hat{f}_\ell(x) = \sum_{i=1}^\ell \alpha_i k(x, x_i)$ for some $\alpha = (\alpha_i)_{i=1}^\ell$, and thus (1) reduces to a finite-dimensional optimization over α .

For the square loss, the optimal α is a solution to $(K + \gamma I)\alpha = y$, where K is the kernel matrix defined by $K_{ij} = k(x_i, x_j)$, I is the identity matrix, and y is the vector of training labels. We now discuss extensions of Tikhonov Regularization that are based on semi-supervised learning assumptions.

MANIFOLD SMOOTHNESS AND CLUSTER ASSUMPTIONS

The input space \mathcal{X} often has a natural distance metric, such as the Euclidean distance when $\mathcal{X} = \mathbb{R}^d$. However, the input points themselves often suggest a different metric. For instance, suppose the input points lie on a one-dimensional manifold, as shown in Figure 1(a). While the points A and C are close in Euclidean distance, they are far apart along the manifold. In Figure 1(b), the manifold has two disjoint components, and while points on different components may be close in Euclidean distance, they are infinitely far apart along the manifold. The idea that the input distribution $P_{\mathcal{X}}$ may live on a low-dimensional manifold in \mathcal{X} is supported by many real-world problems. For example, in speech production, the articulatory organs can be modeled as a collection of tubes whose lengths and widths smoothly parameterize the low-dimensional manifold of speech signals. In vision, the images we get when viewing an object from different positions in \mathbb{R}^3 form a three-dimensional manifold in image space. The manifold smoothness assumption in SSL is that f_* is “smooth” with respect to the manifold underlying $P_{\mathcal{X}}$. Although we don’t generally know $P_{\mathcal{X}}$, in SSL we have a “point cloud” x_1, \dots, x_n sampled from $P_{\mathcal{X}}$. The intrinsic neighborhood structure of the manifold is approximated by the nearest neighbor graph on the point cloud. Let W be the adjacency matrix and define $\Omega_{\mathcal{X}}(f) = (1/2) \sum_{i,j} W_{ij} (f(x_i) - f(x_j))^2$. We can write this intrinsic smoothness measure as a quadratic form with the Laplacian matrix L of the graph, i.e., $\Omega_{\mathcal{X}}(f) = f^T L f$, where $f = (f(x_1) \dots f(x_n))^T$ and $L = D - W$, where D is the diagonal degree matrix $D_{ii} = \sum_j W_{ij}$. We attain the MR algorithm by adding $\Omega_{\mathcal{X}}(f)$ to the objective function of (1):

$$\hat{f}_\ell = \arg \min_{f \in \mathcal{H}} \hat{R}_\ell(f) + \gamma \|f\|_{\mathcal{H}}^2 + \gamma_{\mathcal{X}} \Omega_{\mathcal{X}}(f). \tag{2}$$

As we make $\gamma_{\mathcal{X}}$ large, we push \hat{f}_ℓ towards the region of \mathcal{H} with small $\Omega_{\mathcal{X}}(f)$, i.e., towards those functions with high intrinsic smoothness. As we restrict \hat{f}_ℓ to a subset of \mathcal{H} , we reduce the estimation error. If our manifold smoothness assumption is correct, then $\Omega_{\mathcal{X}}(f_*)$ should also be small, and the restriction will not increase approximation error.

MULTIVIEW ASSUMPTIONS

In the multiview approach to SSL, we have several classes of prediction functions, or “views.” This terminology arises in contexts where an input $x \in \mathcal{X}$ can be decomposed naturally as $x = (x^1, \dots, x^m)$, where each x^i represents a different view of the input x . With this decomposition of the input vector, we can define m views, where the i th view is a class of functions depending only on x^i and ignoring the other components of x . For example, suppose an input x is a clip from a video of a conference room. We divide x into an audio stream and a video stream, which we write as $x = (x^{\text{aud}}, x^{\text{vid}})$. Define our first view, \mathcal{F}^{aud} , to consist of prediction functions of the form $x \mapsto f(x^{\text{aud}})$, and our second view, \mathcal{F}^{vid} , to consist of functions of the form $x \mapsto f(x^{\text{vid}})$. Suppose the goal is to identify who is speaking in each video clip. Although it is

certainly easier to identify who is speaking by using the x^{aud} and x^{vid} signals together, a person who is familiar with the voices and appearances of the individuals in the conference room could do quite well with just one of these signals. Thus it is reasonable to assume that each of our views, both \mathcal{F}^{aud} and \mathcal{F}^{vid} , contains a function that makes the correct predictions. Now suppose we have a very limited amount of training data, and the only time that Bob spoke, there was an accompanying sound of a truck passing outside in the audio stream x^{aud} but no corresponding signal in the video track x^{vid} . Without additional information, it would be difficult to rule out a prediction function $f_{\text{bad}}^{\text{aud}} \in \mathcal{F}^{\text{aud}}$ that identifies Bob as the speaker whenever a truck passes. However, there is no evidence for a truck passing in the video signal, and thus there is no function in \mathcal{F}^{vid} that can consistently make the same predictions as $f_{\text{bad}}^{\text{aud}}$. Since we assumed that each view contains a function that makes the correct predictions, and \mathcal{F}^{vid} does not contain any function that matches $f_{\text{bad}}^{\text{aud}}$, we can conclude that $f_{\text{bad}}^{\text{aud}}$ does not make the correct predictions. Thus by using the assumption that each view has a good function, we can prune out functions, such as $f_{\text{bad}}^{\text{aud}}$, that fit the training data but will not perform well in general. To effect this pruning in practice, we introduce a coregularization function $\Omega_C(f^1, f^2)$ that measures the disagreement between f^1 and f^2 . Then, we solve

$$\begin{aligned} (\hat{f}_\ell^1, \hat{f}_\ell^2) = \arg \min_{f^1 \in \mathcal{H}^1, f^2 \in \mathcal{H}^2} & \hat{R}_\ell \left(\frac{1}{2} (f^1 + f^2) \right) \\ & + \gamma_1 \|f^1\|_{\mathcal{H}^1}^2 + \gamma_2 \|f^2\|_{\mathcal{H}^2}^2 \\ & + \lambda \Omega_C(f^1, f^2), \end{aligned} \tag{3}$$

for RKHSs \mathcal{H}^1 and \mathcal{H}^2 . The final prediction function is $\hat{\phi}_\ell(x) = (\hat{f}_\ell^1(x) + \hat{f}_\ell^2(x))/2$. Taking $\Omega_C(f^1, f^2) = \sum_{i=1}^n (f^1(x_i) - f^2(x_i))^2$, we get the CoRLS [7], [3], [6] algorithm.

SOLUTION

MULTIVIEW POINT CLOUD REGULARIZATION

We now consider a generalized Tikhonov regularization framework that subsumes the methods discussed above. Our views

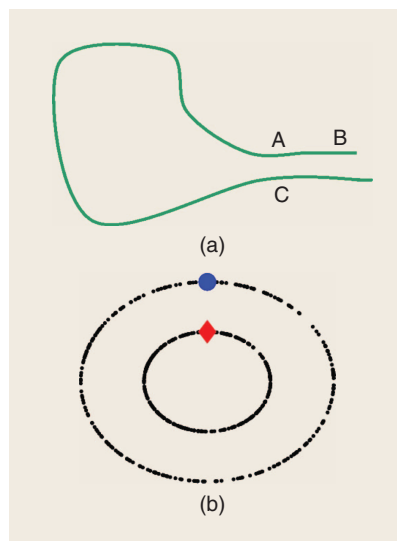


[FIG1] (a) One connected component and (b) two connected components.

are RKHSs $\mathcal{H}^1, \dots, \mathcal{H}^m$ of real-valued functions on \mathcal{X} , with kernels k^1, \dots, k^m , respectively. Define $\mathcal{F} = \mathcal{H}^1 \times \dots \times \mathcal{H}^m$. We want to select one function from each view, say $f = (f^1, \dots, f^m) \in \mathcal{F}$, and to combine these functions into a single prediction function. We fix a vector of view weights $\mathbf{a} = (a_1, \dots, a_m) \in \mathbb{R}^m$, and define $u(f) = a_1 f^1 + \dots + a_m f^m$. The final prediction function is $\phi(x) = u(f)(x) = a_1 f^1(x) + \dots + a_m f^m(x)$. We define the space of these prediction functions by $\tilde{\mathcal{H}} = u(\mathcal{F})$. Note that $\tilde{\mathcal{H}}$ may change with different settings of \mathbf{a} , in particular when entries of \mathbf{a} are set to zero. For any $f \in \mathcal{F}$, we denote the column vector of function evaluations on the point cloud by $\underline{f} = (f^1(x_1), \dots, f^1(x_n), \dots, f^m(x_1), \dots, f^m(x_n))^T \in \mathbb{R}^{mn}$. (For the rest of this article, we use bold face to indicate a finite dimensional column vector and an underline to indicate that a vector is the concatenation of a column vector associated with each of the m views.) For any positive semidefinite (PSD) matrix $M \in \mathbb{R}^{mn \times mn}$, the objective function for MVPCR is

$$\begin{aligned} \arg \min_{\phi \in \tilde{\mathcal{H}}} \min_{\{(f^1, \dots, f^m) : a_1 f^1 + \dots + a_m f^m = \phi\}} \hat{R}_\ell(\phi) \\ + \sum_{i=1}^m \gamma_i \|f^i\|_{\tilde{\mathcal{H}}^\ell}^2 + \lambda \underline{f}^T M \underline{f}, \end{aligned} \quad (4)$$

where $\gamma_1, \dots, \gamma_m > 0$ are RKHS norm regularization parameters, and $\lambda \geq 0$ is the point cloud norm regularization parameter. In the objective function above, $\tilde{\mathcal{H}}$ is a raw set of functions, without any additional structure. The main result of this article endows $\tilde{\mathcal{H}}$ with an RKHS structure.

THEOREM 1

There exists an inner product for which $\tilde{\mathcal{H}}$ is an RKHS with norm

$$\|\phi\|_{\tilde{\mathcal{H}}} = \sqrt{\min_{\{f : u(f) = \phi\}} \left[\sum_{i=1}^m \gamma_i \|f^i\|_{\tilde{\mathcal{H}}^\ell}^2 + \lambda \underline{f}^T M \underline{f} \right]} \quad (5)$$

and reproducing kernel function

$$\begin{aligned} \tilde{\mathcal{K}}(z, x) = \sum_{j=1}^m \frac{a_j^2}{\gamma_j} k^j(z, x) - \lambda \underline{k}_x^T A G^{-1} \\ \times (I + \lambda M G^{-1} \mathcal{K})^{-1} M G^{-1} A \underline{k}_z, \end{aligned} \quad (6)$$

where we denote the point cloud kernel matrix for the j th view by $K^j = (k^j(x_i, x_k))_{i,k=1}^n$, \mathcal{K} is defined as the block diagonal matrix $\mathcal{K} = \text{diag}(K^1, \dots, K^m) \in \mathbb{R}^{mn \times mn}$,

$$\begin{aligned} \underline{A} = \text{diag} \left(\underbrace{a_1, \dots, a_1}_{n \text{ times}}, \dots, \underbrace{a_m, \dots, a_m}_{n \text{ times}} \right) \\ \underline{G} = \text{diag} \left(\underbrace{\gamma_1, \dots, \gamma_1}_{n \text{ times}}, \dots, \underbrace{\gamma_m, \dots, \gamma_m}_{n \text{ times}} \right), \end{aligned}$$

and we denote the column vector of kernel evaluations between the point cloud and an arbitrary point $x \in \mathcal{X}$, for each kernel, by $\underline{k}_x = (k^1(x_1, x), \dots, k^1(x_n, x), \dots, k^m(x_1, x), \dots, k^m(x_n, x))^T$.

For a proof, we point the reader to [5], where this theorem was first presented. We call the kernel given in (6) the multiview kernel. This theorem implies that the solution to the MVPCR problem in (4) is exactly the solution to the standard RKHS regularization problem of (1) over RKHS $\tilde{\mathcal{H}}$. We use this reduction below to derive complexity and generalization bounds for MVPCR as a consequence of well-known results for RKHS learning. This approach is much simpler than the “bare-hands” proof used for the special case of CoRLS in [6]. From an algorithmic perspective, since we have an explicit form for the multiview kernel, we can easily plug it in to any standard kernel algorithm. For example, the kernel can be plugged into kernel logistic regression, Bayesian kernel methods such as Gaussian processes, one-class SVMs, kernel PCA, etc., turning these algorithms into multiview learners. We note that Theorem 1 generalizes the result of [8] for MR and of [9] for CoRLS.

SUPERVISED LEARNING, MR, COMR, AND OTHER SPECIAL CASES

It is easy to see that if we consider a single view, i.e., $m = a_1 = 1$, and set $\lambda = 0$, we get back the basic RKHS regularization problem of (1). If we take $\lambda > 0$ and M to be the graph Laplacian, then we get back MR. To get CoRLS, we take $m = 2$, $a_1 = a_2 = 1/2$, and set M to the matrix

$$M_C := \begin{pmatrix} I & -I \\ -I & I \end{pmatrix},$$

where each I is an $n \times n$ identity matrix. We can easily extend coregularization to m views by taking M_C to be an $m \times m$ block matrix with $n \times n$ identity matrices on the diagonal, and $n \times n$ negative identity matrices off the diagonal. In particular, this recovers the multiview generalization of coregularization with the least squares loss given in [3]. In [10], a kernel matrix is derived for coregularized Gaussian processes. Their approach is transductive and does not provide predictions for points outside of the unlabeled training set. The multiview kernel presented here (for $M = M_C$) not only recovers their kernel matrix when evaluated on the point cloud but also possesses a natural out-of-sample extension to unseen data points. In addition, it generalizes to other loss functions, gives explicit control over view weights and can incorporate more general data-dependent regularizers than the typical ℓ_2 -disagreement.

RADEMACHER COMPLEXITY AND GENERALIZATION BOUNDS

In the section “Problem Setting,” we discussed how we can trade off between approximation error and estimation error by changing the size of \mathcal{F} . We now discuss a precise measure of function class size. For a class of functions \mathcal{F} and a distribution on the domain \mathcal{X} , the empirical Rademacher complexity of \mathcal{F} for a sample $x_1, \dots, x_\ell \in \mathcal{X}$ is defined as $\hat{\mathfrak{N}}_\ell(\mathcal{F}) = \mathbb{E} \sup_{f \in \mathcal{F}} (1/\ell) \sum_{i=1}^{\ell} \sigma_i f(x_i)$, where the expectation is over the i.i.d. Rademacher variables $\sigma_1, \dots, \sigma_\ell$, which are distributed as $P(\sigma_i = 1) = P(\sigma_i = -1) = 1/2$. For fixed σ_i s, the supremum selects the function $f \in \mathcal{F}$ that best “fits” the σ_i s, in the sense that when $\sigma_i = 1$, $f(x_i)$ is a large positive number, and when $\sigma_i = -1$, $f(x_i)$ is a large negative number. Thus if $\hat{\mathfrak{N}}_\ell(\mathcal{F})$ is large, then \mathcal{F} has functions that can fit most random noise sequences and may be prone to over-fitting the data. We make this statement precise with a well-known generalization bound [2], which bounds the worst case gap between risk and empirical risk in terms of $\hat{\mathfrak{N}}_\ell(\mathcal{F})$.

THEOREM 2

Suppose that the loss function $V(\cdot, y)$ is L -Lipschitz for every $y \in \mathbf{R}$ and $V(\cdot, \cdot) \in [a, b]$ for some $a < b$. Then for any $\delta \in (0, 1)$, with probability at least $1 - \delta$, $\sup_{f \in \mathcal{F}} |\hat{R}_\ell(f) - R(f)| \leq 2L\hat{\mathfrak{N}}_\ell(\mathcal{F}) + (b - a) \sqrt{2 \log(3/\delta)/\ell}$

We now derive bounds for MVPCR. It is straightforward to show that if $\hat{\varphi}_\ell$ is an MVPCR solution, then $\|\hat{\varphi}_\ell\|_{\tilde{\mathcal{H}}}^2 \leq r^2 := \hat{R}_\ell(0)$, where the zero denotes the prediction function that always predicts zero. Thus we can consider the optimization in MVPCR to be over the norm ball $\tilde{\mathcal{H}}_r$ of radius r , rather than over all of $\tilde{\mathcal{H}}$. By a well-known result, $\hat{\mathfrak{N}}_\ell(\tilde{\mathcal{H}}_r) \leq r/\ell \sqrt{\text{tr } \tilde{K}}$, where \tilde{K} is the kernel matrix for $\tilde{\mathcal{K}}$ on the labeled training points (see [5] and references therein). To apply Theorem 2, $\tilde{\mathcal{H}}_r$ must be a fixed class of functions. However, in our setting $\tilde{\mathcal{H}}_r$ may be a random class of functions, even depending on the labeled data via the point cloud. Let us assume that the point cloud defining $\tilde{\mathcal{H}}$ is independent of the labeled data points. Then conditional on the point cloud, $\tilde{\mathcal{H}}_r$ is a deterministic class of functions. Plugging the bound on $\hat{\mathfrak{N}}_\ell(\tilde{\mathcal{H}}_r)$ into Theorem 2, we attain a generalization bound for any MVPCR algorithm. This also implies a bound on estimation error, since $R(\hat{f}_\ell) - R(f^*) \leq 2 \sup_{f \in \mathcal{F}} |\hat{R}_\ell(f) - R(f)|$, which is bounded by Theorem 2.

UNLABELED DATA IMPROVES THE BOUND

Here we present a result that shows how unlabeled data reduces the Rademacher complexity, and thus reduces the bound on estimation error, for the specific case of two-view CoRLS. Recall that the parameter λ controls the extent to which we enforce agreement between the prediction functions from each view: f^1 and f^2 . Let $\tilde{\mathcal{H}}(\lambda)$ denote the space of prediction functions for a particular value of λ . It has been shown in [9] and [6] that the Rademacher complexity for a ball of radius r in $\tilde{\mathcal{H}}(\lambda)$ decreases with λ by an amount determined by $\Delta(\lambda) = \sum_{i=1}^{\ell} \rho^2(\gamma_1^{-1} k_{U_i}^1, \gamma_2^{-1} k_{U_i}^2)$, where $k_{U_i}^1$ and $k_{U_i}^2$ are $u \times 1$ column vectors whose j th entries are $k^1(x_i, x_{\ell+j})$ and $k^2(x_i, x_{\ell+j})$, respectively, and $\rho(\cdot, \cdot)$ is

a metric on the space \mathbf{R}^u defined by $\rho^2(s, t) = \lambda(s - t)' (I + \lambda S)^{-1} (s - t)$, where $S = \gamma_1^{-1} K_{UU}^1 + \gamma_2^{-1} K_{UU}^2$ is a weighted sum of the unlabeled data kernel matrices. We see that the complexity reduction $\Delta(\lambda)$ grows with the ρ -distance between the two different (scaled) representations of the labeled points, where the measure of distance is determined by the unlabeled data.

MANIFOLD COREGULARIZATION

As an application of MVPCR, we present manifold coregularization (CoMR), a multiview version of MR. Roughly speaking, CoMR is two-view CoRLS with a particular choice of views. The ambient view, denoted by \mathcal{H}^A , is an RKHS of functions defined on the input space \mathcal{X} . As usual, the “smoothness” of a function $f \in \mathcal{H}^A$ is measured by the RKHS norm $\|f\|_{\mathcal{H}^A}$. The intrinsic view, denoted by \mathcal{H}^I , comprises functions whose domain is restricted to the point cloud $\mathcal{M} = \{x_1, \dots, x_n\}$. The measure of smoothness for a function $f \in \mathcal{H}^I$ is taken to be $\Omega_{\mathcal{I}}(f) = f^T M_{\mathcal{I}} f$, where $M_{\mathcal{I}}$ is a PSD matrix, such as the Laplacian matrix of the data adjacency graph. While in MR we look for a single function $f \in \mathcal{H}$ that has both small RKHS norm and small $\Omega_{\mathcal{I}}(f)$, in CoMR we look for two separate functions, an $f^I \in \mathcal{H}^I$ with small $\Omega_{\mathcal{I}}(f)$ and an $f^A \in \mathcal{H}^A$ with small norm. We then ask only that f^A and f^I be close, as measured by a coregularization term. Due to the difference in representations caused by differences in ambient and geodesic distances, by the discussion above we expect good reductions in the complexity of our coregularized function space $\tilde{\mathcal{H}}$. For CoMR, we define the view combination function as $u(f^A, f^I) = a^A f^A + a^I f^I$, for any fixed $a^A, a^I \in \mathbf{R}$, and we define the space of final prediction functions as $\tilde{\mathcal{H}} = \{u(f^A, f^I) \mid f^A \in \mathcal{H}^A, f^I \in \mathcal{H}^I\}$. Then the CoMR optimization problem is written as: $\arg \min_{\varphi \in \tilde{\mathcal{H}}} \min_{(f^A, f^I) \in u^{-1}(\varphi)} \hat{R}_\ell(\varphi) + \gamma_A \|f^A\|_{\mathcal{H}^A}^2 + \gamma_{\mathcal{I}} (f^I)^T M_{\mathcal{I}} f^I + \lambda f^T M_C f$, where $f = (f^A(x_1), \dots, f^A(x_n), f^I(x_1), \dots, f^I(x_n))^T$, and where M_C , as before, is the coregularization matrix for two views. If $M_{\mathcal{I}}$ is invertible, or if we make it so by adding a small

ridge term, then \mathcal{H}^I is a finite-dimensional RKHS with norm $\|f^I\|_{\mathcal{I}} = \sqrt{(f^I)^T M_{\mathcal{I}} f^I}$ and kernel function $k: \mathcal{M} \times \mathcal{M} \rightarrow \mathbf{R}$ given by the matrix $(M_{\mathcal{I}})^{-1}$. Thus our two views are proper RKHSs, and we may directly apply Theorem 1 to get an expression for a multiview kernel on \mathcal{M} . Experiments in [9] showed that CoMR with $a^I = a^A = 1/2$ significantly outperforms MR on several learning tasks. Note that if $a^I \neq 0$, then the final prediction function will only be defined on \mathcal{M} , since f^I is itself restricted to \mathcal{M} . However, if we take $a^I = 0$, our final prediction function will be f^A , which is defined on all of \mathcal{X} . For this special case, the CoMR objective function can be written more simply as $\arg \min_{f^A \in \mathcal{H}^A} \hat{R}_\ell(f^A) + \gamma_A \|f^A\|_{\mathcal{H}^A}^2 + \gamma_{\mathcal{I}} (f^A)^T M_{\mathcal{I}} (I + (\gamma_{\mathcal{I}}/2\lambda) M_{\mathcal{I}})^{-1} f^A$. When we take $\lambda \rightarrow \infty$, the objective function reduces to MR. As $\lambda \rightarrow 0$, the dependence on the unlabeled data vanishes as the last term in the objective function goes to zero. Thus λ mediates between purely supervised learning at one limit and MR at the other limit. Note that when $a^I = 0$, CoMR may be viewed as MR with a modified smoothness measure. See [5] for more details.

CONCLUSION

We have presented a new RKHS where Tikhonov regularization incorporates both smoothness and multiview semi-supervised assumptions, and subsumes manifold regularization and coregularization as special cases. Compared with early frameworks, MVPCR gives prediction functions with out-of-sample extensions, handles multiple views, and allows for arbitrary linear combinations of individual views, rather than simple averages. We expect that the multiview kernel will allow convenient “plug-and-play” exploration of novel semisupervised algorithms, both in terms of implementation and performance bounds.

AUTHORS

David S. Rosenberg (drosen@stat.berkeley.edu) is with Sense Networks, New York.

(continued on page 150)

and tradeoff, are discussed in Chapters 8, 9, and 10.

Finally, the third part (Chapter 11 to Chapter 18) of this book explores the applications of cooperation beyond the physical layer, including content-aware cooperative multiple access protocols at the link layer, distributed cooperative routing at the network layer, cross-layer design based on source-channel coding with cooperation, and coverage expansion and the network lifetime maximization via cooperation.

One topic that this reviewer believes could have been better addressed in this book was hierarchical cooperation. In Chapter 4, the authors describe the linear capacity scaling achieved by hierarchical cooperation in a wireless ad hoc network. In this reviewer's opinion, this topic would have benefited from its own targeted background section. For example, defining capacity scaling and explaining its importance in wireless networks would have been beneficial for an audience of nonexperts. Further, in this chapter, the authors do not discuss the underlying propagation model and other assumptions involved in the network modeling when they review Gupta and Kumar's result for aggregate throughput scaling limitations. Generally, this reviewer believed that this material was not connected well with the previous sections of this chapter that focus on the outage capacity

performance for the small-scale fading channel, and that the exposition could have been improved by connecting it to better to the rest of the chapter.

This book has many distinctive features that make it attractive both as a textbook and as a reference. The depth of the discussions varies throughout the book. At the beginning of the text, the authors have made a significant effort to introduce the basic concepts behind radio propagation, the capacity of wireless channels, the various diversity techniques to combat fading, as well as the state-of-the-art OFDM and MIMO techniques. This allows a beginner to build up the requisite foundation easily. The material related to cooperative communications is presented in a coherent and integrated fashion. The authors describe different schemes to implement cooperation, analyze these algorithms through evaluating the outage capacity and characterizing diversity gains, and summarize the tradeoff between system performance and operation complexity. This helps readers develop a broad understanding of the topic and obtain a comprehensive knowledge of the principles behind various methods. There are also sufficient references, concise chapter summaries, and bibliographical notes for readers seeking more details.

In terms of aesthetics and functionality, the book is very well designed. The formatting, font, and figures are all well

laid out and organized, making the book easy to read. The figures in the book are quite attractive. Key examples are set out from the rest of the text by lined boxes.

Cooperative Communications and Networking is likely to be positioned between the book *Cooperative Communications* by Gerhard Kramer, Ivana Maric, and Roy D. Yates and the book *Wireless Communications* by Andrea Goldsmith. The former book has a narrower focus and can be viewed as a tutorial for the reader who is familiar with information theoretic concepts. The latter book provides a general discussion on current wireless systems, such as equalization, coding for wireless systems, diversity, multiple antennas communications, and spread spectrum. Compared with these two books, *Cooperative Communications and Networking* fills a slightly different market need. In particular, Liu, Sadek, Su and Kwasinski's book provides a more thorough treatment of material that is at the cutting edge of cooperative communication over wireless network, and its treatment of cooperative communication is more advanced. Overall, *Cooperative Communications and Networking* is an excellent, reader-friendly book. This reviewer believes that this book will have a lasting impact upon those involved in cooperative communications research. **SP**

Vikas Sindhwani (vsindh@us.ibm.com) is with IBM Research.

Peter L. Bartlett (bartlett@cs.berkeley.edu) is with the Computer Science Division and Department of Statistics, University of California, Berkeley.

Partha Niyogi (niyogi@cs.uchicago.edu) is with the Department of Computer Science, University of Chicago.

REFERENCES

[1] M. Belkin, P. Niyogi, and V. Sindhwani, "Manifold regularization: A geometric framework for learning

from labeled and unlabeled examples," *J. Mach. Learn. Res.*, vol. 7, pp. 2399–2434, Nov. 2006.

[2] O. Bousquet, S. Boucheron, and G. Lugosi, "Introduction to statistical learning theory," *Advanced Lectures on Machine Learning*. Berlin: Springer, 2004.

[3] U. Brefeld, T. Gärtner, T. Scheffer, and S. Wrobel, "Efficient co-regularized least squares regression," in *Proc. ICML*, 2006, vol. 23, pp. 137–144.

[4] P. Niyogi, "Manifold regularization and semi-supervised learning: Some theoretical analyses," Tech. Rep., Dept. Comput. Sci., Univ. Chicago, TR-2008-01, Chicago, IL, 2008.

[5] D. S. Rosenberg, "Semi-supervised learning with multiple views," Ph.D. dissertation, Univ. California, Berkeley, 2008.

[6] D. S. Rosenberg and P. L. Bartlett, "The Rademacher complexity of co-regularized kernel

classes," in *Proc. Int. Conf. Artificial Intelligence and Statistics*, Mar. 2007, pp. 396–403.

[7] V. Sindhwani, P. Niyogi, and M. Belkin, "A co-regulation approach to semi-supervised learning with multiple views," in *Proc. Workshop Learning with Multiple Views, ICML*, 2005, pp. 74–79.

[8] V. Sindhwani, P. Niyogi, and M. Belkin, "Beyond the point cloud: From transductive to semi-supervised learning," in *Proc. ICML*, vol. 119, 2005, pp. 824–831.

[9] V. Sindhwani and D. S. Rosenberg, "An RKHS for multi-view learning and manifold co-regularization," in *Proc. Int. Conf. Machine Learning*, July 2008, pp. 976–983.

[10] S. Yu, B. Krishnapuram, R. Rosales, H. Steck, and B. R. Rao, "Bayesian co-training," in *Proc. NIPS 20*. Cambridge, MA: MIT Press, 2008, pp. 1665–1672. **SP**